Role of the different copper species on the activity of Cu/zeolite catalysts for SCR of NO_x with NH_3

Unai De La Torre[1], Beñat Pereda-Ayo[1], Juan R. González-Velasco[1,*], María José Illán-Gómez[2], Agustin Bueno-López[2].

[1]Departamento de Ingeniería Química, Facultad de Ciencia y Tecnología, Universidad del País Vasco, UPV/EHU, Campus de Leioa, P. O. Box 644, ES-48080 Bilbao, Bizkaia, Spain

[2]Department of Inorganic Chemistry. University of Alicante. Carretera de San Vicente s/n. E03080, Alicante (Spain)

Abstract

The SCR of NO_x with NH_3 has been studied by using different Cu zeolite catalysts, prepared both with ZSM5 and BETA zeolite supports by ionic exchange or by impregnation. The catalysts were characterized by ICP-AES, N_2 adsorption at -196 ºC, XRD, TEM, XPS and H_2-TPR. The catalysts characterization confirmed the presence of different Cu(II) species on all catalyst (CuO and Cu(II) exchanged on tetrahedral and octahedral positions of the zeolites framework). Clear evidences of Cu(I) or Cu(0) species were not obtained. CuO was more abundant in high copper-content catalysts and in ZSM5 catalysts, due to its lower ionic exchange capacity, while isolated Cu(II) ions are more abundant in low copper-content catalysts and in BETA catalysts. It was concluded that CuO catalyzes the oxidation of NO to NO_2, and this favors the reduction of NO_x at lower temperature (the NH_3-NO_2 reaction is faster than the NH_3–NO reaction because NO_2 is much more oxidizing than NO), whereas isolated Cu(II) ions maintain high NO_x conversion at high temperatures.

Keywords: SCR, NO_x removing, Cu-zeolite, Cu cluster

* Corresponding author:
Juan R. González-Velasco
Dept. Chemical Engineering
University of the Basque Country
P.O. Box 644, ES-48980 Bilbao, Spain
E-mail: juanra.gonzalezvelasco@ehu.es

1. Introduction

It is well recognized that the use of diesel and lean burn engines decreases the fuel consumption and thereby reduces the CO_2 emissions. However, conventional three way catalysts (TWC) are not capable to reduce nitrogen oxides (NO_x) from diesel engines due to the excess of oxygen in the exhaust. In the last decade, one of the main approaches proposed for NO_x reduction in diesel exhausts has been the selective catalytic reduction (SCR).

SCR was originally developed for stationary emission sources, mainly power plants [1]. However, it soon turned out to be a promising technology for the NO_x removal in automobile applications as well [2]. In 2005 it was introduced for commercial heavy-duty vehicles in Europe, and more recently also for passenger cars. The NH_3-SCR converter needs an external source of the selective reducing agent, e.g. urea. The urea solution is injected in a controlled way into the exhaust line, where it is thermally decomposed into NH_3 and CO_2. The ammonia then reacts selectively with NO_x under lean (oxidising) conditions, giving N_2 as the final product [3]. Non-noble metals like copper, iron and cerium supported on ZSM5 and BETA zeolite are among the most active catalysts for the urea/NH_3-SCR process [4-7], among others like copper/chabazite catalysts [8,9].

Cu(II) ion-exchanged ZSM5 (Cu-ZSM5) zeolites were first tested, showing high NO decomposition rates and NO_x SCR activities [10]. More recently, Cu(II)-exchanged BETA zeolites (Cu-BETA) have shown a good activity for the NH_3-SCR of NO_x, but they present better hydrothermal stability than similar ZSM5 catalysts [11]. Burch et at. [12] identified the presence of Cu(I) species under reaction conditions, and proposed that Cu(I) is the main active species for the reaction. Whatever, it is generally accepted that both copper ions (Cu(II) and/or Cu(I)), which exist in the exchange sites of ZSM5, play an important role in the reaction of NH_3-SCR. In the last decade, a lot of research has been performed to obtain information about the nature of the copper active sites for this process [13-17].

Nevertheless, there is still an open discussion concerning the chemical and mechanistic aspects involved in SCR, mainly those related with the role of the different copper species exchanged or placed on the zeolite. In our previous work [18], we have analysed the NH_3-SCR catalytic performance of different ZSM5 and BETA supported catalysts, varying the preparation method and copper content. We found that while ZSM5 supported catalysts achieved better NO_x conversion in a low temperature range (250-350 °C), BETA supported catalysts were active at higher temperature (350-450 °C). On the other hand, an increase in the copper content and the use of an impregnation preparation method (vs. the ion exchange) allows achieving higher NO_x conversion at lower temperatures but it decreases at intermediate and higher temperatures.

The aim of this work is to understand the role of the different copper species on the activity of Cu/zeolite catalysts in the NH_3-SCR process for NO_x removal in a wide temperature range (140–500 °C). For characterization of the different Cu-zeolite catalysts, which were prepared by both impregnation and ion-exchange methods, XPS, H_2-TPR and TEM techniques have been used.

2. Experimental

2.1. Catalysts preparation.

The SCR catalysts consisted of copper-supported zeolites. Fresh zeolites were supplied by Zeolyst International, namely CP414E (BETA, Si/Al=12.5) and CBV5524G (ZSM5, Si/Al=25). The zeolites were first calcined at 550 ºC for 4 h to obtain the acid form. The catalysts were prepared by two different conventional procedures: ion exchange (IE) and wetness impregnation (IM). Metal ion exchange was carried out by dissolving the required amount of $Cu(COOCH_3)_2$ (Panreac, 98%) in water. Then, H-ZSM5 or H-BETA was added to this solution (8 g/L) and it was stirred for 24 h at 65 ºC. The ion exchanged zeolites were then filtered, washed twice with deionized water, dried overnight at 110 ºC and calcined at 550 ºC for 4 h.

On the other hand, the wetness impregnation method consisted of adding slowly the required amount of the copper precursor dissolved in water (1.5 wt.%) at 40 ºC and 3 mm Hg to 6 grams of H-BETA or H-ZSM5, under continuous rotation until the solvent was evaporated. The samples were dried overnight at 110 ºC and calcined at 550 ^{o}C for 4 h.

All the catalysts were then pelletized, crushed and sieved to 0.3-0.5 mm. Previous experiments carried out with different particle size catalysts revealed that mass transfer limitations were not controlling the reaction kinetics for a particle size of 0.3-0.5 mm.

The most relevant details of the preparation procedure of copper-zeolite catalysts, as well as the nomenclature used are summarized in Table 1. For each support, BETA or ZSM5, four catalysts were prepared, three by ion exchange and one by wetness impregnation. With regards to the ion exchange catalysts, increasing copper concentration solutions (160, 320, 640 and 2000 ppm) were used in order to obtain different copper loading on the zeolitic support.

TABLE 1

2.2. Characterization techniques.

ICP-AES. The actual amount of copper in the prepared catalysts was determined by ICP-AES, after metal extraction from the solid samples with 1:2 HNO_3:HF mixture at 90 ºC, which assures complete samples dissolving.

N_2 adsorption. The BET surface area of the zeolite samples were determined by N_2 adsorption at −196 °C using a Micromeritics ASAP 2020 equipment.

XR Diffraction (XRD). The crystalline structure of the copper modified zeolite samples were analyzed by XRD (Philips PW1710 diffractometer). The samples were finely ground and X-Ray diffractograms were recorded with copper Kα radiation in continuous scan mode from 5 to 80° of 2θ with 0.02° per second sampling interval. PANalytical X'pert HighScore specific software was used for data treatment. JCPDS database was used to interpret the diffractograms.

X Ray Photoelectronic Spectroscopy (XPS). XPS characterization was carried out in a VG-Microtech Multilab electron spectromenter using Mg-Kα (1254.6 eV) radiation source. To obtain the XPS spectra, the pressure of the analysis chamber was maintained at $5 \cdot 10^{-10}$ mbar. The binding energy (BE) scale was adjusted by setting the carbon 1s transition at 284.6 eV. The XPS measurements were performed in the electron binding energy ranges corresponding to copper 2p, oxygen 1s, silicon 2p, aluminum 2p and carbon 1s core excitations [19, 20].

Transmission Electron Microscopy (TEM). A JOEL (JEM-2010) microscope was used to obtain TEM images of the catalysts. Few droplets of an ultrasonically dispersed suspension of each sample in ethanol were placed on a copper grid with lacey carbon film and dried at ambient conditions for TEM characterizations. In order to obtain particle size distribution of copper, around 200 copper particles were identified and measured.

Hydrogen Temperature Programmed Reduction (H_2-TPR). Reducibility of copper catalysts was investigated by TPR using H_2. The samples were pretreated in 30 ml/min of 10% O_2/He mixture gas flow at 550 ºC for 45 min and then cooled down to 30 ºC and flushed out with helium for 60 min. Then the samples were heated from room temperature to 600 ºC with 10 °C/min ramp in a 60 ml/min of 5% H_2/Ar mixture gas flow. The water formed during reduction with H_2 was trapped using a cold trap and the hydrogen consumption was continuously monitored with a TCD detector.

2.3. SCR experiments.

The SCR experiments were performed in a down flow stainless steel reactor. The reactor tube, with 1 g of 0.3-0.5 mm pelletized Cu-zeolite SCR catalyst inside, was located into a 3-zone tube furnace. The temperature was measured by a thermocouple at the top of the catalyst bed. The reaction temperature was varied from 100 to 500 ºC in steps of 40 ºC. The composition of the feed gas mixture was 750 ppm NO, 750 ppm NH_3 and 9.5% O_2 using Ar as the balance gas. Gases were fed via mass flow controllers and the total flow rate was set at 3000 ml·min^{-1}, which corresponded to a space velocity (GHSV) of 90,000 h^{-1}. The experimental set-up was designed to minimize the gas phase oxidation of NO to NO_2, and therefore, the NO_2 concentration in the gas fed is almost null. The NO, NO_2 NH_3 and N_2O concentrations at the reactor exit were monitored every 40 ºC, once the analysis has been stabilized for at least 10 min, by an online FTIR multigas analyzer (MKS 2030).

The NO (X_{NO}) and NH_3 (X_{NH3}) conversions were calculated as

$$X_{NO} = \frac{F_{NO}^{in} - F_{NO_x}^{out}}{F_{NO}^{in}} \times 100 \quad (1)$$

$$X_{NH_3} = \frac{F_{NH_3}^{in} - F_{NH_3}^{out}}{F_{NH_3}^{in}} \times 100 \quad (2)$$

and the N_2 (S_{N2}), NO_2 (S_{NO2}) and N_2O (S_{N2O}) selectivities were calculated as

$$S_{N_2} = \frac{2F_{N_2}^{out}}{F_{NH_3}^{in}X_{NH_3}+F_{NO}^{in}X_{NO}} \times 100 \quad (3)$$

$$S_{NO_2} = \frac{F_{NO_2}^{out}}{F_{NH_3}^{in}X_{NH_3}+F_{NO}^{in}X_{NO}} \times 100 \quad (4)$$

$$S_{N_2O} = \frac{2F_{N_2O}^{out}}{F_{NH_3}^{in}X_{NH_3}+F_{NO}^{in}X_{NO}} \times 100 \quad (5)$$

where F_i represents the concentration of the "i" specie and the superscripts "in" and "out" indicate that the gas concentration was measured at the inlet and the exit of the reactor, respectively.

3. Results and Discussion.

3.1 Analysis of the copper content and surface area of the catalysts.

Figure 1 shows the copper loading of the different catalysts prepared by ionic exchange with regard to the initial copper concentration on the water solutions used for the exchange process. An auxiliary continuous line has been included which represents the maximum copper loading that would be achieved if all copper available in the water solutions were incorporated into the zeolites. Furthermore, two auxiliary dot lines represent the maximum amount of copper that can be exchanged on each zeolite. The Si/Al ratios and the corresponding molecular composition of the ZSM5 and BETA zeolites (Table 1) predict these maxima amounts of copper are 2 and 5.6 wt. %, respectively, considering that one Cu(II) cation needs two ionic exchange sites.

FIGURE 1

All data on Figure 1 lie below the concentration predicted by the auxiliary continuous line corresponding to maximum copper loading, evidencing that there is copper left in the water solutions after the exchange processes. The amount of copper loaded on both zeolites increases with copper concentration in the water solution, and as a general trend, the amount of copper loaded on the ZSM5 zeolite is lower to that loaded on BETA zeolite (for similar exchange conditions). This is in agreement with the Si/Al ratios and with the exchange capacity of each zeolite. The copper loading on the BETA zeolite catalysts increases with the copper concentration on the water solution until total consumption of the exchange sites on the B-IE-5.8 catalyst. On the contrary, some Cu-ZSM5 catalysts exceed the 100 % exchange level, and this can be due either to the formation of copper dimers in solution $(Cu^{2+}OH^{-})_2$, which would result in the anchoring of two Cu(II) ions per exchangeable site [21], and/or to the formation of extraframework copper species. During the ion exchange, local changes in pH could promote copper hydroxide precipitation [22].

In spite of this observation, the X ray diffractograms of the copper-exchanged zeolites, which are not shown for the sake of brevity, did not present neither peaks corresponding to metallic copper (Cu^0) nor to copper oxide (CuO), evidencing high copper dispersion in all cases. Besides, the diffractograms of the acid and copper exchanged zeolites are quite similar, which means that the crystalline structure of the zeolites was not apparently modified after the copper incorporation.

Figure 2 shows the BET surface area of the catalysts as a function of the copper loading. Fresh BETA and ZSM5 zeolites presented BET surface areas of 532 and 474 $m^2 \cdot g^{-1}$, respectively. These areas decrease linearly, with almost the same slope, with the copper content. This decrease of BET surface area can be attributed to the partial pores blockage by copper species and/or to the destruction of micropores during copper loading due to aluminum leaching by acid attack [23]. The surface area decrease observed for the impregnated catalysts (B-IM-1.3 and Z-IM-1.2) are not in line with their counterparts prepared by ion-exchange, and impregnated catalysts show a much higher decrease in the BET surface area. This suggests that pore blockage by copper species is the main reason of the BET surface area decrease.

FIGURE 2

3.2 Analysis of the copper particle size by TEM.

The copper particle size distributions on the different catalysts have been determined by TEM. As an example, Figures 3a and 3b show TEM images of the lowest and highest copper content ZSM5 catalysts, whereas Figures 3c and 3d show the counterpart BETA catalysts, all of them prepared by ionic exchange.

FIGURE 3

As expected, the amount and size of the dark spots, mainly attributed to CuO as it will be demonstrated afterwards, depends both on the nature of the zeolite and on the copper loading. A major number of dark spots are observed for high-copper content catalysts (Z-IE-4.9 and B-IE-5.8, Figures 3b and 3d) than for the counterpart low-copper content catalysts, and BETA catalysts only shows small particles (diameter $<$ 1.5 nm) while ZSM5 presents both small and large particles.

Figure 4 shows the copper particle size distribution for all catalysts. No relevant differences were detected in the copper size distribution among catalysts prepared by impregnation and ionic exchange.

FIGURE 4

As a general trend, BETA catalysts present narrower particle size distribution than ZSM5 catalysts, with particle sizes centered on 1 nm and most particles being smaller than 4 nm. Only the highest-copper content BETA catalyst (B-IE-5.8) shows few copper particles larger than 10 nm. ZSM5 catalysts exhibit wider particle size distributions than BETA catalysts, and a considerable amount of large particles, especially for high copper loading catalyst, were identified. Few of these particles achieved sizes even higher than 300 nm.

These observations are in good agreement with the conclusions of the previous section, where it was observed that copper is mainly exchanged on zeolite sites of the BETA support while an important fraction of the metal loaded on ZSM5 is impregnated rather than exchanged (see Figure 1 and previous section). These differences are consistent with the Si/Al ratio and ionic exchange capacity of both zeolites. However, it is important to pay especial attention to the Z-IE-1.4 sample, since large CuO particles are observed in the TEM images but the total ionic exchange capacity has not been achieved (see Table 1). This suggests that not only the ionic exchange capacity (or the Si/Al ratio) of the zeolites plays a role on the nature of the copper species formed, but also the zeolite structure seems to be involved. The framework types of the BETA and ZSM5 zeolites are BEA and MFI, respectively, and the accessible volumes of these structures are 23 and 10 % respectively [24]. Also, the maximum diameter of a sphere that can enter into these structures is 6.68 Å for BEA and 6.36 Å for MFI. According to this, the copper solution used for the ionic exchange is expected to enter more easily into the BETA zeolite porosity than on the ZSM5 porosity, and therefore, a smaller particle size distribution of the CuO particles is obtained in the BETA zeolite catalysts.

3.3 Analysis of the copper species nature by XPS and H_2-TPR.

In order to study the surface composition of the catalysts and the nature of the surface copper species, XPS characterization was carried out. A certain amount of carbon was detected by XPS on the surface of all catalysts, close to 10% in some cases, and for this reason a direct analysis of the quantitative results of the surface composition is complex and comparison of elements ratio is more meaningful. In Table 2, the Si/Al surface ratios are compiled together with the ratio between surface copper (determined by XPS) and total copper (determined by ICP) contents.

TABLE 2

The Si/Al surface ratio decreases by increasing the copper loading both for BETA and ZSM5 catalysts. This can be attributed to the decrease of the solutions pH by increasing the Cu(II) precursor concentration, which favors the zeolites dealumination [23]. This aluminum leaching would result in a certain accumulation of aluminum species on the crystals surface.

The ratio between surface and total copper contents ($Cu_{surface}/Cu_{total}$) provides information about the metal loading process. Constant ratios (0.42) were obtained for BETA zeolite catalysts prepared by ionic exchange and a quite similar value was obtained by impregnation of this support (0.37 for B-IM-1.3). These values below 1 indicate that copper is mainly accumulated into the zeolite porosity, and support that copper cations are actually exchanged on the zeolite sites [25]. The similar values obtained by the impregnation and ionic exchange loading methods suggest that copper could be exchanged even in the impregnated BETA catalyst. For ZSM5 catalysts prepared by ionic exchange, the $Cu_{surface}/Cu_{total}$ ratio increases with the copper loading and most values are higher than those obtained with the counterpart BETA zeolite catalysts. This is in line with the worst copper dispersion obtained on the ZSM5 zeolite support. Note that higher particles were observed by TEM on ZSM5 zeolite catalysts (see Figures 3 and 4). This worst dispersion of copper can be attributed to the higher Si/Al ratio, and therefore lower cation exchange capacity, of the ZSM5 zeolite with regard to that of the BETA zeolite and to the more accessible porosity of the BETA zeolite. The $Cu_{surface}/Cu_{total}$ ratio obtained with the ZSM5 zeolite impregnated with copper (Z-IM-1.2 catalyst) is higher than values obtained by ionic exchange of this zeolite, which is an evidence of worst dispersion in this case.

Figures 5a and 5b show the X ray photoelectronic spectra corresponding to the copper 2p transition for Cu-ZSM5 and Cu-BETA catalysts, respectively. It is usually reported that Cu(2$p^{3/2}$) transition appears at energy values lower than 933 eV for metallic copper (Cu^0) and Cu_2O (Cu(I)), while it shifts to values higher than 933 eV for Cu(II) species [26]. According to this assignation, all profiles included on Figure 5 are consistent with the presence of different Cu(II) species. The presence of the shake-up satellite (not shown in Figure 5) appearing in all catalysts with energies 10 eV higher than the Cu(2$p^{3/2}$) transition also gives evidences of the presence of Cu(II). However, the energy of the Cu(2$p^{3/2}$) transition does not allow unequivocally identify the oxidation states of copper [23], and for the proper identification of the oxidation state of the copper species the Auger peak must be taken into account. The Auger parameter (α), which is calculated as the sum of copper 2p binding energy and Auger peak kinetic energy, has been included in Table 3. The values of the Auger parameter of most catalysts are well above 1850 eV, and these values confirm the presence of Cu(II) cations. Only the Z-IE-4.9 catalyst presents Auger values below 1850 eV, and this could be due to the formation of bulk CuO instead of Cu(II) cations exchanged on the zeolite framework and/or to the presence of Cu(I) cations, but the formation of CuO seems to be more reasonable [27].

TABLE 3

FIGURE 5

The Cu(2$p^{3/2}$) transition included on Figure 5 can be deconvoluted in three main contributions located around 933.2 eV, 934.0 eV and 936.0 eV. As discussed, all these contributions can be most likely be attributed to different Cu(II) species [19]. The band located at ca. 933.2 eV is tentatively assigned to agglomerated CuO particles present on the surface [28], while second and third peaks located at ca. 934.0 and 936.0 eV are thought to correspond to isolated Cu(II) species with different coordination, as was evidenced by Hajjar et al. [29] by FTIR and MQMAS NMR. The peak at 934.0 eV corresponds to isolated Cu(II) in tetrahedral coordination, while the peak appearing at 936.0 correspond to isolated Cu(II) in octahedrical coordination [28], which is related to the presence of two kinds of exchange sites in the zeolites framework. As isolated Cu(II) in octahedrical coordination are more strongly attached to the zeolite framework, the corresponding contribution appears at the highest binding energy followed by isolated Cu(II) in tetrahedral coordination and finally agglomerated Cu(II) species which appear at the lowest binding energy.

The contribution of each individual transition to the total intensity of the Cu(2$p^{3/2}$) band depends both on the zeolite type and on the copper content. As a general trend, increasing copper content leads to an increase in the contribution located at lowest binding energy, i.e. 933.2 eV (dashed red line) to the detriment of that located at 934.0 eV (dashed green line), while the third one located at 936.0 eV (dashed blue line) remains constant for Cu-ZSM5 and increases for Cu-BETA. The areas of these contributions were calculated and expressed as a percentage of the total Cu(2$p^{3/2}$) transition in Table 3.

Note that the increasing contribution of the peak located at 933.2 eV, indicating the presence of agglomerated CuO particles, increases with the copper loading: 13% of the total Cu(2$p^{3/2}$) transition for Z-IE-1.4, 31 % for Z-IE-2.6 and 53 % for Z-IE-4.9. Meanwhile, the contribution of isolated Cu(II) in tetrahedral coordination shows a reverse relationship respect to the amount of agglomerated particles, decreasing with increasing the copper content, i.e. 78 % for Z-IE-1.4, 59 % for Z-IE-2.6 and 38 % for Z-IE-4.9. The contribution of isolated Cu(II) in octahedrical coordination is almost constant, around 9 %, regardless the copper loading. Thus, it can be suggested that copper first preferentially occupies the ion exchange sites and, once those are saturated, CuO is accumulated on the zeolite surface. Agglomerated CuO particles are more abundant in ZSM5 zeolite than on BETA zeolite if catalysts with similar copper loading are compared. For instance, the signal attributed to CuO particles represents 53 % in Z-IE-4.9 catalysts while it results in just 34 % for B-IE-5.8, although the copper loading is even higher for the latter. This fact could be related to the higher Si/Al ratio, and therefore lower cation exchange capacity, of the ZSM5 zeolite with regard to that of the BETA zeolite and to the more accessible porosity of the BETA zeolite, which promotes the formation of CuO aggregates for high copper loadings. Finally, XPS does not show significant differences between ion exchanged and impregnated samples, which reveals that the proportion of each copper species on the surface is only influenced by the copper amount and the zeolite type.

Additional information about the nature of the different copper species in the catalysts was obtained by Temperature Programmed Reduction experiments (H_2-TPR), and Figure 6 shows the H_2 consumption profiles. The copper-free H-zeolites did not contain reducible ions and no H_2 consumption was noticed; therefore, all H_2 consumed by the catalysts can be attributed to the reduction of copper cations. It is important to mention that the H_2-TPR profiles obtained with fresh catalysts (Figure 6) and after the SCR experiments (not shown) did not show significant changes, confirming that copper remains mainly oxidized even after the SCR experiments. This is not surprising taking into account the highly oxidizing nature of the simulated diesel exhaust gas stream.

FIGURE 6

All the catalysts consumed H_2 due to the reduction of Cu(II), and the higher the copper content of the catalysts, the higher the H_2 consumption [30]. Considering the

ICP-AES copper content, the amount of catalyst used in the H_2-TPR experiments and the stoichiometry of the following reactions:

$CuO + H_2 \rightarrow Cu + H_2O$ (for bulk CuO particles) (6)

$Cu(II)\text{-zeolite} + H_2 \rightarrow Cu + (2H^+)\text{-zeolite}$ (for Cu(II) cations exhanged on the zeolites)(7)

a H_2/Cu=1 ratio should be obtained if all copper were Cu(II) and if all Cu(II) species were completely reduced to metal copper. According to the H_2/Cu ratios obtained experimentally (0.9-1.0 in all cases), all the catalysts accomplish these hypotheses. This confirms that only Cu(II) species exist on the catalysts, which is consistent with the XPS results.

All the profiles included in Figure 6 are composed by several maxima and shoulders indicating, in line with the XSP results, the presence of copper species with different reducibility. The maximum that appears around 250 °C for most of the catalysts corresponds to the reduction of bulk CuO species, which are more easily reduced than exchanged Cu(II) ions [31]. A shoulder at lower temperatures, which is related with the reduction of the CuO particles surface, is observed in some profiles, and its contribution increases with the total copper content. The CuO reduction maximum/shoulder observed in the H_2-TPR profiles would be associated to the copper 2p XPS contribution at 933.2 eV (see Figure 5 and Table 3).

The H_2-consumption peaks appearing at higher temperatures can be assigned to Cu(II) cations exchanged on the zeolite, which need more temperature to be reduced than CuO. The presence of different exchanged Cu(II) cations is consequence of the existence of different kinds of framework sites in ZSM5 and BETA zeolites [29]. The peaks with a maximum at temperatures around 350 °C for ZSM5 catalysts and around 450 °C for BETA catalyst, corresponds to the most easily reduced exchanged Cu (II) species [31]. According to the XPS results, this peak could be related with the reduction of tetracoordinated Cu(II) species. Finally, the peaks with a maximum at temperatures around 480 °C for ZSM5 catalysts and around 600 °C for BETA catalysts correspond, in line with XPS results, to the reduction of Cu(II) cations in octahedral coordination, which are strongly attached to the zeolite.

As it has been previously reported [30], there is a significant effect of copper loading on the reducibility of the different copper species. From our data it can be confirmed that an increase of the copper loading shifts the reduction peaks to lower temperature. This is consistent with the formation of larger amounts of dimeric copper-species as the copper loading increases [32]. These dimeric copper species contain bridging oxygen atoms that can react with H_2 at comparably lower temperatures than isolated copper-sites. Thus, as expected, the copper dispersion decreases for high copper loading.

In addition to the qualitative assignation of the H_2-reduction peaks to the different copper species in the catalyst, a semi-quantitative analysis of the H_2-consumption profiles can be done. The highest temperature peaks (assigned to Cu(II) cations exchanged on octahedral sites) are the most intense peaks for the low copper content catalysts. This indicates that the octahedral sites are first exchanged. The intensity of the peaks assigned to Cu(II) cations exchanged on tetrahedral sites grows appreciably with the copper content, becoming more intense than the third contribution (the one assigned to Cu(II) cations exchanged on octahedral sites). This confirms that the tetra-coordinated sites are occupied by Cu(II) cations after the octahedral sites, and that the amount of tetrahedral sites available on the zeolites is higher to that of octahedral sites. Finally, the most intense H_2-reduction peak of the ZSM5 catalyst with highest copper content (Z-IE-4.9) is assigned to CuO reduction, confirming that bulk copper oxide formation is favored once the exchange sites have been occupied. On the contrary, the position and intensity of the H_2-reduction peaks of B-IE-5.8 suggest that

Cu(II) exchanged on tetrahedral positions is the most abundant copper species on the highest copper content BETA catalyst. This is consistent with the lower Si/Al ratio, and therefore higher ionic exchange capacity, of the BETA zeolite with regard to that of the ZSM5 zeolite, and to the more accessible porosity of the BETA zeolite.

As a summary, the XPS and H_2-TPR characterization confirm the presence of different Cu(II) species on the catalyst, namely, CuO and Cu(II) exchanged on tetrahedral and octahedral positions of the zeolite framework. Clear evidences of Cu(I) or Cu(0) species were not obtained in any case. As a general trend, Cu(II) exchanged on octahedral positions prevails for catalysts with low copper content, and the exchange of Cu(II) on tetrahedral positions and the formation of CuO is progressively favored by increasing the copper content. The formation of CuO is more important on the ZSM5 zeolite than on BETA due to the higher Si/Al ratio, and therefore lower ionic exchange capacity, of the former, and to the more accessible porosity of the BETA zeolite.

3.4. SCR experiments.

Figures 7a and 7b show the NO_x and NH_3 conversions and Figures 7c, 7d and 7e show the selectivity towards N_2, NO_2 and N_2O, respectively, as a function of the reaction temperature in SCR experiments.

FIGURE 7

The behavior of any catalyst is qualitatively similar, and the obtained catalytic results are typical of NO_x SCR reactions in all cases. NO conversions increased with temperature because the NH_3-NO_x reactions are promoted, reaching a maximum conversion for an intermediate temperature and decreasing afterwards as the oxidation of ammonia with O_2 is favored at high temperature [33, 34]. The NH_3 conversions also increased with temperature, but 100% conversion was maintained above a certain temperature because the NH_3-O_2 reaction prevails. The minimum temperature for 100% ammonia conversion is the same at which the maximum NO conversion is achieved. Regardless the catalyst, N_2 is the main nitrogen-reaction product (above 80% selectivity in the whole range of temperatures studied for all catalyst) and few N_2O and/or NO_2 are only detected.

The particular behavior of the catalysts depends on the zeolite nature, on the copper content and on the copper loading procedure. The lowest NOx conversions were obtained with the impregnated catalysts, and this could be a consequence of the partial blockage of the zeolite network by copper species, as deduced from the BET values (see Figure 2). The partial blockage of the zeolite pores is expected to force the reactions to preferentially occur on the external surface of the crystals, hindering the access of gases to the internal copper sites.

For catalysts prepared with the same zeolite, the NO and NH_3 conversion curves are shifted to lower temperatures as the copper content increases, while the N_2O and NO_2 selectivities slightly increase. As discussed in the previous characterization sections, the presence of CuO is favored for high copper contents, and this would explain these catalytic trends. A tentative explanation is that CuO catalyzes the oxidation of NO to NO_2, and this favors the reduction of NO_x at lower temperature since the NH_3-NO_2 reaction is faster than the NH_3–NO reaction (NO_2 is much more oxidizing than NO). The formation of NO_2 is only evident at high temperature, once the selectivity of the NH_3-NO_x reactions decrease, because in the range of temperatures of high NO reduction selectivity the NO_2 potentially formed is expected to react with NH_3, and consequently, is not detected.

The low-copper content catalysts, and mainly those prepared by ionic exchange and with BETA zeolite, have a better catalytic behavior at high temperature than the high-copper content counterparts. For instance, at 425 ºC, the catalyst B-IE-2.1 reached the highest NO conversion among all catalysts, keeping low NO_2 and N_2O production. This catalyst has a high proportion of exchanged Cu(II) species (mainly Cu(II) exchanged on octahedral sites), and this type of copper cations seems to be responsible of the activity at high temperature. It can be concluded that CuO clusters, which are more abundant in high copper-content catalysts, promote NO reduction at low temperature whereas isolated Cu(II) ions, which are more abundant in low copper-content catalysts, maintained high NO_x conversion even at high temperatures. In addition, catalysts with low CuO content exhibit higher N_2 selectivity, which was progressively reduced by increasing the copper loading. In those cases, the selectivity of the reaction moved towards N_2O and NO_2.

Comparing the supports, it can be observed that Cu-ZSM5 catalysts are more active at low temperature whereas Cu-BETA catalysts maintain higher activity at high temperature. This behavior can also be related to the nature of the copper species present in each catalyst. As a general trend, there are higher amounts of CuO on ZSM5 catalysts than on BETA catalysts due to the higher Si/Al ratio, and therefore lower ionic exchange capacity, of the ZSM5 zeolite, and to the more accessible porosity of the BETA zeolite, which favors the formation of exchanged Cu(II) species with regard to bulk CuO particles.

4. Conclusions.

In this study, the SCR of NO_x with NH_3 has been studied with different copper zeolite catalysts and the following conclusions have been achieved:

The catalysts characterization confirmed the presence of different Cu(II) species in all catalyst, namely, CuO and Cu(II) exchanged on tetrahedral and octahedral positions of the zeolite framework. Clear evidences of Cu(I) or Cu(0) species were not obtained in any case. As a general trend, Cu(II) exchanged on octahedral positions prevails for catalysts with low copper content, and the exchange of Cu(II) on tetrahedral positions and the formation of CuO is progressively favored by increasing the copper content.

CuO is more abundant in high copper-content catalysts and in ZSM5 catalysts, while isolated Cu(II) ions are more abundant in low copper-content catalysts and in BETA catalysts. There are higher amounts of CuO on ZSM5 catalysts than on BETA catalysts due to the lower ionic exchange capacity of the ZSM5 zeolite.

The nature of the copper species affects the SCR behavior of the studied catalysts. CuO clusters promote NO reduction at low temperature whereas isolated Cu(II) ions maintain high NO_x conversion at high temperatures. In addition, catalysts with low CuO content exhibit higher N_2 selectivity, since CuO promotes the formation of N_2O and NO_2.

It is suggested that CuO catalyzes the oxidation of NO to NO_2, and this favors the reduction of NO_x at lower temperature since the NH_3-NO_2 reaction is faster than the NH_3–NO reaction (NO_2 is much more oxidizing than NO).

Acknowledgements.

Authors wish to acknowledge the financial support provided by the Spanish Ministry of Economy and Competitiveness (CTQ2012-30703), the Basque Government (IT-657-13) and the UPV/EHU (UFI 11/39). One of the authors (UDLT) wants to acknowledge to the Basque Government for the PhD Research Grant (BFI-2010-330).

REFERENCES

[1] P. Forzatti, L. Lietti, E. Tronconi, Nitrogen Oxides Removal Industrial, in: Encyclopedia of Catalysis, John Wiley & Sons, Inc., 2002.

[2] R.M. Heck, R.J. Farrauto, S.T. Gulati, Diesel Engine Emissions, in: Catalytic Air Pollution Control, John Wiley & Sons, Inc., 2009, pp. 238-294.

[3] P. Forzatti, L. Lietti, I. Nova, E. Tronconi, Diesel NOx aftertreatment catalytic technologies: Analogies in LNT and SCR catalytic chemistry, Catalysis Today. 151 (2010) 202-211.

[4] L. Lietti, I. Nova, E. Tronconi, P. Forzatti, Transient kinetic study of the SCR-DeNOx reaction, Catalysis Today. 45 (1998) 85-92.

[5] E.C. Corbos, M. Haneda, X. Courtois, P. Marecot, D. Duprez, H. Hamada, Cooperative effect of Pt–Rh/Ba/Al and CuZSM-5 catalysts for NOx reduction during periodic lean-rich atmosphere, Catalysis Communications. 10 (2008) 137-141.

[6] N. Wilken, K. Wijayanti, K. Kamasamudram, N.W. Currier, R. Vedaiyan, A. Yezerets, L. Olsson, Mechanistic investigation of hydrothermal aging of Cu-Beta for ammonia SCR, Applied Catalysis B: Environmental. 111–112 (2012) 58-66.

[7] A. Corma, V. Forne´s, E. Palomares, Selective catalytic reduction of NOx on Cu-beta zeolites, Applied Catalysis B: Environmental. 11 (1997) 233-242.

[8] S. T. Korhonen, D. W. Fickel, R. F. Lobo, B. M. Weckhuysen, A. M. Beale, Chemical Communications. 47 (2011), 800-802.

[9] S. J. Schmieg, S. H. Oha, C. H. Kima, D. B. Brown, J. H. Lee, C. H.F. Peden, D. H. Kim. Catalysis Today 184 (2012) 252– 261.

[10] A. Grossale, I. Nova, E. Tronconi, D. Chatterjee, M. Weibel, The chemistry of the NO/NO2–NH3 “fast” SCR reaction over Fe-ZSM5 investigated by transient reaction analysis, Journal of Catalysis. 256 (2008) 312-322.

[11] S. Brandenberger, O. Kroecher, A. Tissler, R. Althoff, The State of the Art in Selective Catalytic Reduction of NOx by Ammonia Using Metal-Exchanged Zeolite Catalysts, Catalysis Reviews-Science and Engineering. 50 (2008) 492-531.

[12] R. Burch, P.J. Millington, Role of propene in the selective reduction of nitrogen monoxide in copper-exchanged zeolites, Applied Catalysis B: Environmental. 2 (1993) 101-116.

[13] G.D. Lei, B.J. Adelman, J. Sárkány, W.M.H. Sachtler, Identification of copper(II) and copper(I) and their interconversion in Cu/ZSM-5 De-NOx catalysts, Applied Catalysis B: Environmental. 5 (1995) 245-256.

[14] R. Pirone, P. Ciambelli, G. Moretti, G. Russo, Nitric oxide decomposition over Cu-exchanged ZSM-5 with high Si/Al ratio, Applied Catalysis B: Environmental. 8 (1996) 197-207.

[15] B. Modén, P. Da Costa, B. Fonfé, D.K. Lee, E. Iglesia, Kinetics and Mechanism of Steady-State Catalytic NO Decomposition Reactions on Cu–ZSM5, Journal of Catalysis. 209 (2002) 75-86.

[16] J. Dědeček, L. Čapek, B. Wichterlová, Nature of active sites in decane-SCR-NOx and NO decomposition over Cu-ZSM-5 zeolites, Applied Catalysis A: General. 307 (2006) 156-164.

[17] G. Moretti, C. Dossi, A. Fusi, S. Recchia, R. Psaro, A comparison between Cu-ZSM-5, Cu–S-1 and Cu–mesoporous-silica–alumina as catalysts for NO decomposition, Applied Catalysis B: Environmental. 20 (1999) 67-73.

[18] U. De La Torre, B. Pereda-Ayo, J.R. González-Velasco, Cu-zeolite NH3-SCR catalysts for NOx removal in the combined NSR–SCR technology, Chem. Eng. J. 207–208 (2012) 10-17.

[19] V.I. Pârvulescu, P. Grange, B. Delmon, NO decomposition over physical mixtures of Cu-ZSM-5 with zeolites or oxides, Applied Catalysis B: Environmental. 33 (2001) 223-237.

[20] V.K. Kaushik, R.P. Vijayalakshmi, N.V. Choudary, S.G.T. Bhat, XPS studies on cation exchanged zeolite A, Microporous and Mesoporous Materials. 51 (2002) 139-144.

[21] L.O. Öhman, B. Ganemi, E. Björnbom, K. Rahkamaa, R.L. Keiski, J. Paul, Catalyst preparation through ion-exchange of zeolite Cu-, Ni-, Pd-, CuNi- and CuPd-ZSM-5, Mater. Chem. Phys. 73 (2002) 263-267.

[22] G. Centi, S. Perathoner, Nature of active species in copper-based catalysts and their chemistry of transformation of nitrogen oxides, Applied Catalysis A: General. 132 (1995) 179-259.

[23] B.M. Abu-Zied, Cu2+-acetate exchanged X zeolites: Preparation, characterization and N2O decomposition activity, Microporous and Mesoporous Materials. 139 (2011) 59-66.

[24] http://www.iza-online.org/ Access on August 2013.

[25] A. Corma, A. Palomares, F. Márquez, Determining the Nature of the Active Sites of Cu-Beta Zeolites for the Selective Catalytic Reduction (SCR) of NOx by Using a Coupled Reaction-XAES/XPS Study, Journal of Catalysis. 170 (1997) 132-139.

[26] www.lasurface.com, accessed on 7th May 2013.

[27] M. Fernández-García, E. Gómez Rebollo, A. Guerrero Ruiz, J.C. Conesa, J. Soria, Influence of Ceria on the Dispersion and Reduction/Oxidation Behaviour of Alumina-Supported Copper Catalysts, Journal of Catalysis. 172 (1997) 146-159.

[28] J.F. Xu, W. Ji, Z.X. Shen, S.H. Tang, X.R. Ye, D.Z. Jia, X.Q. Xin, Preparation and Characterization of CuO Nanocrystals, Journal of Solid State Chemistry. 147 (1999) 516-519.

[29] R. Hajjar, Y. Millot, P.P. Man, M. Che, S. Dzwigaj, Two Kinds of Framework Al Sites Studied in BEA Zeolite by X-ray Diffraction, Fourier Transform Infrared Spectroscopy, NMR Techniques, and V Probe, Journal of Physical Chemistry C. 112 (2008) 20167-20175.

[30] B. Moden, J.M. Donohue, W.E. Cormier, H.-. Li, Effect of Cu-loading and structure on the activity of Cu-exchanged zeolites for NH3-SCR, in: Studies in Surface Science and Catalysis, Elsevier, pp. 1219-1222.

[31] J. Zhou, Q.-. Xia, S.-. Shen, S. Kawi, K. Hidajat, Catalytic oxidation of pyridine on the supported copper catalysts in the presence of excess oxygen, Journal of Catalysis. 225 (2004) 128-137.

[32] P. Da Costa, B. Moden, G. Meitzner, D. Lee, E. Iglesia, Spectroscopic and chemical characterization of active and inactive Cu species in NO decomposition catalysts based on Cu-ZSM5, Physical Chemistry Chemical Physics. 4 (2002) 4590-4601.

[33] J.H. Kwak, D. Tran, S.D. Burton, J. Szanyi, J.H. Lee, C.H.F. Peden, Effects of hydrothermal aging on NH3-SCR reaction over Cu/zeolites, Journal of Catalysis. 287 (2012) 203-209.

[34] J. Li, H. Chang, L. Ma, J. Hao, R.T. Yang, Low-temperature selective catalytic reduction of NOx with NH3 over metal oxide and zeolite catalysts—A review, Catalysis Today. 175 (2011) 147-156.

Figure Captions.

Figure 1. Relation between the initial copper concentration and the actual copper content (%) in zeolite.

Figure 2. Relation between the actual copper content and BET surface area.

Figure 3. TEM images of (a) Z-IE-1.4, (b) Z-IE-4.9, (c) B-IE-2.1 and (d) B-IE-5.8.

Figure 4. Particle size distribution of catalysts determined from TEM images.

Figure 5. X ray Photoelectric Spectra (copper $2p^{3/2}$ transition) for (a) Cu-ZSM5 catalysts and (b) Cu-BETA catalysts.

Figure 6. H_2-TPR profiles of fresh: a) Cu-BETA catalysts and (b) Cu-ZSM-5 catalysts.

Figure 7. Conversion of NO_x, NH_3 and $N_{2,}$ N_2O and NO_2 selectivity during SCR reaction for (a) BETA and (b) ZSM5 catalysts.

Table 1. Summary of the prepared catalysts

Catalyst nomenclature	Support	Si/Al	Copper loading method	Copper initial concentration in the impregnation solutions (ppm)	Copper content on the catalyst (wt. %)	Exchange sites potentially* occupied by Cu(II) cations (%)
B-IM-1.3	BETA	12.5	Impregnation	-	1.3	23
B-IE-2.1	BETA	12.5	Ion exchange	320	2.1	37
B-IE-2.9	BETA	12.5	Ion exchange	640	2.9	52
B-IE-5.8	BETA	12.5	Ion exchange	2000	5.8	103
Z-IM-1.2	ZSM5	25	Impregnation	-	1.2	59
Z-IE-1.4	ZSM5	25	Ion exchange	160	1.4	69
Z-IE-2.6	ZSM5	25	Ion exchange	640	2.6	129
Z-IE-4.9	ZSM5	25	Ion exchange	2000	4.9	243

Table 2. Results of the surface characterization by XPS.

Catalyst	$Cu_{surface}/Cu_{total}$	Si/Al
Z-IM-1.2	0.78	14
Z-IE-1.4	0.38	14
Z-IE-2.6	0.58	8
Z-IE-4.9	0.64	5
B-IM-1.3	0.37	11
B-IE-2.1	0.42	8
B-IE-2.9	0.42	7
B-IE-5.8	0.42	6

Table 3. XPS characterization of the copper species. Percentage of the different copper species identified in the $Cu2p^{3/2}$ transition and Auger energy.

Catalyst	Peak at 933.2 eV (%)	Peak at 934.0 eV (%)	Peak at 936.0 eV (%)	Auger (eV)
Z-IM-1.2	9	83	8	1865.3
Z-IE-1.4	13	78	8	1865.6
Z-IE-2.6	31	59	10	1865.2
Z-IE-4.9	53	38	9	1848.6
B-IM-1.3	9	79	12	1865.6
B-IE-2.1	16	74	10	1865.5
B-IE-2.9	27	57	16	1865.9
B-IE-5.8	34	45	21	1862.3

Tentative assignation: 933.2 eV corresponds to CuO, 934.0 eV corresponds to isolated Cu(II) in tetrahedral coordination and 936.0 eV corresponds to isolated Cu(II) in octahedrical coordination (see main text for details).

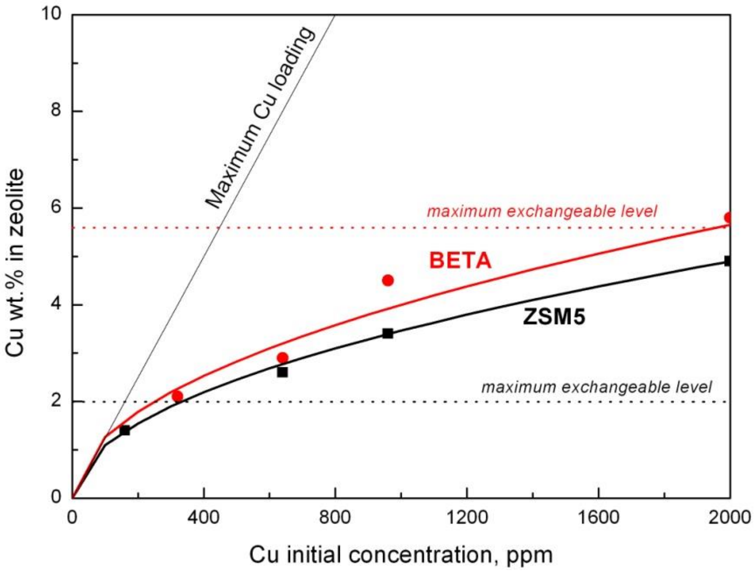
Maximum Cu loading
maximum exchangeable level
BETA
ZSM5
maximum exchangeable level
Cu wt.% in zeolite
Cu initial concentration, ppm
0
2
4
6
8
10
0
400
800
1200
1600
2000

Figure 1

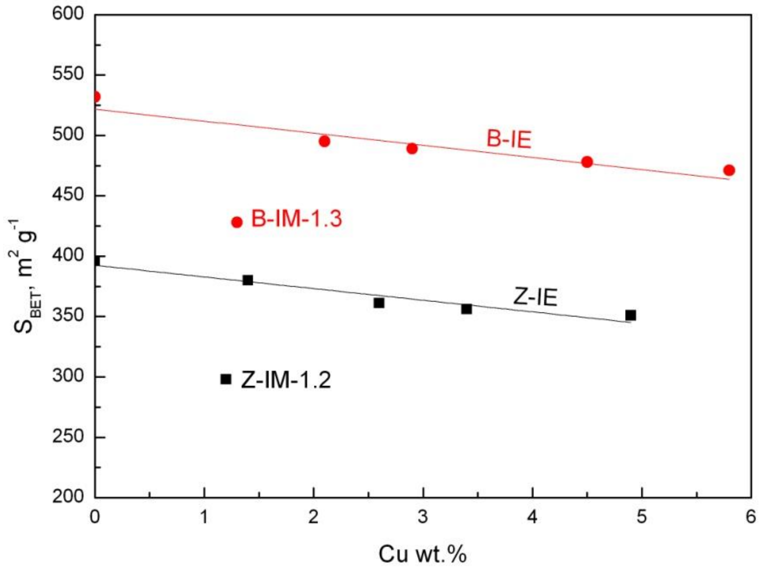
B-IE
B-IM-1.3
Z-IE
Z-IM-1.2
S_BET, m² g⁻¹
Cu wt.%
600
550
500
450
400
350
300
250
200
0
1
2
3
4
5
6

Figure 2

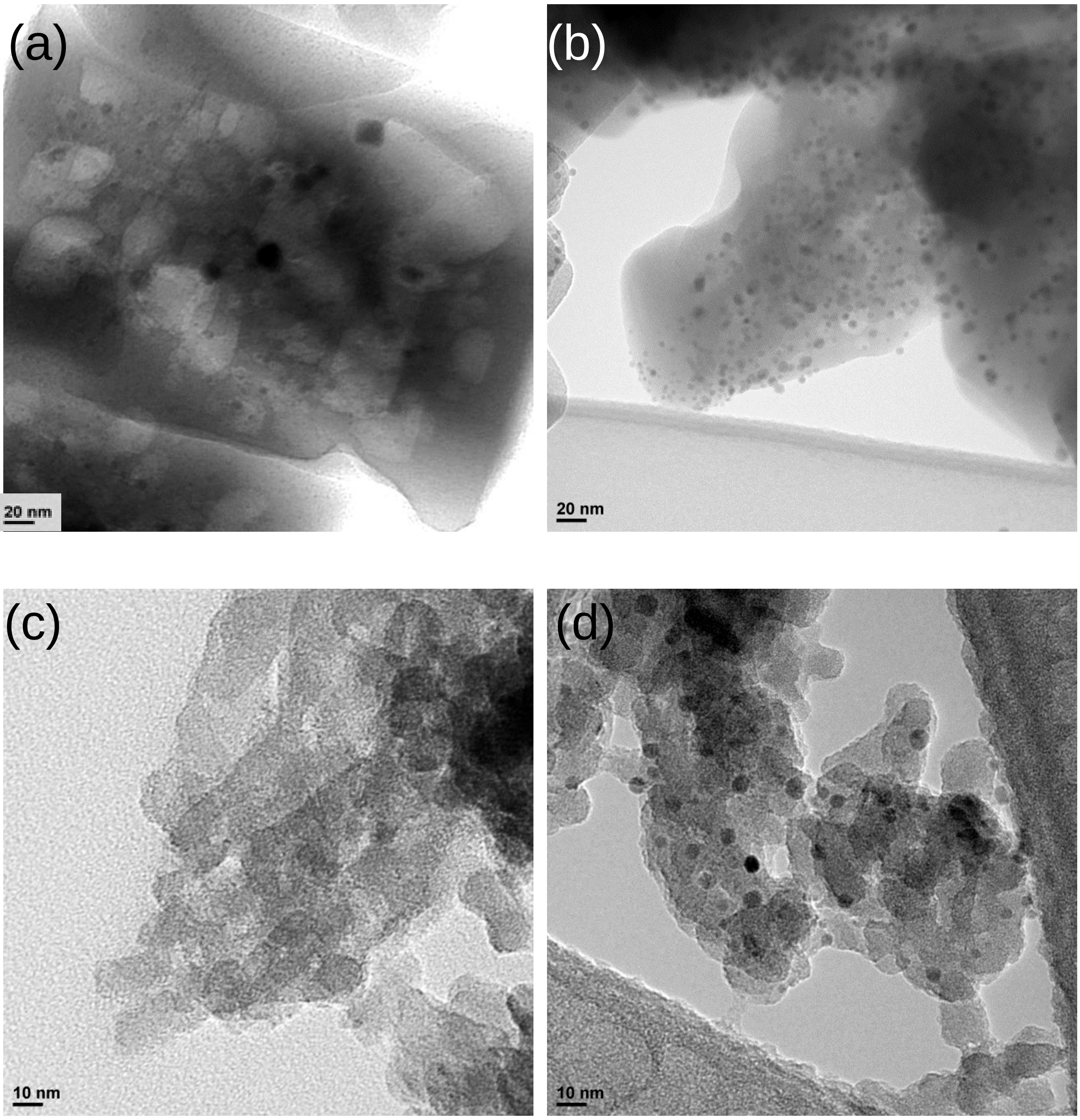

Figure 3

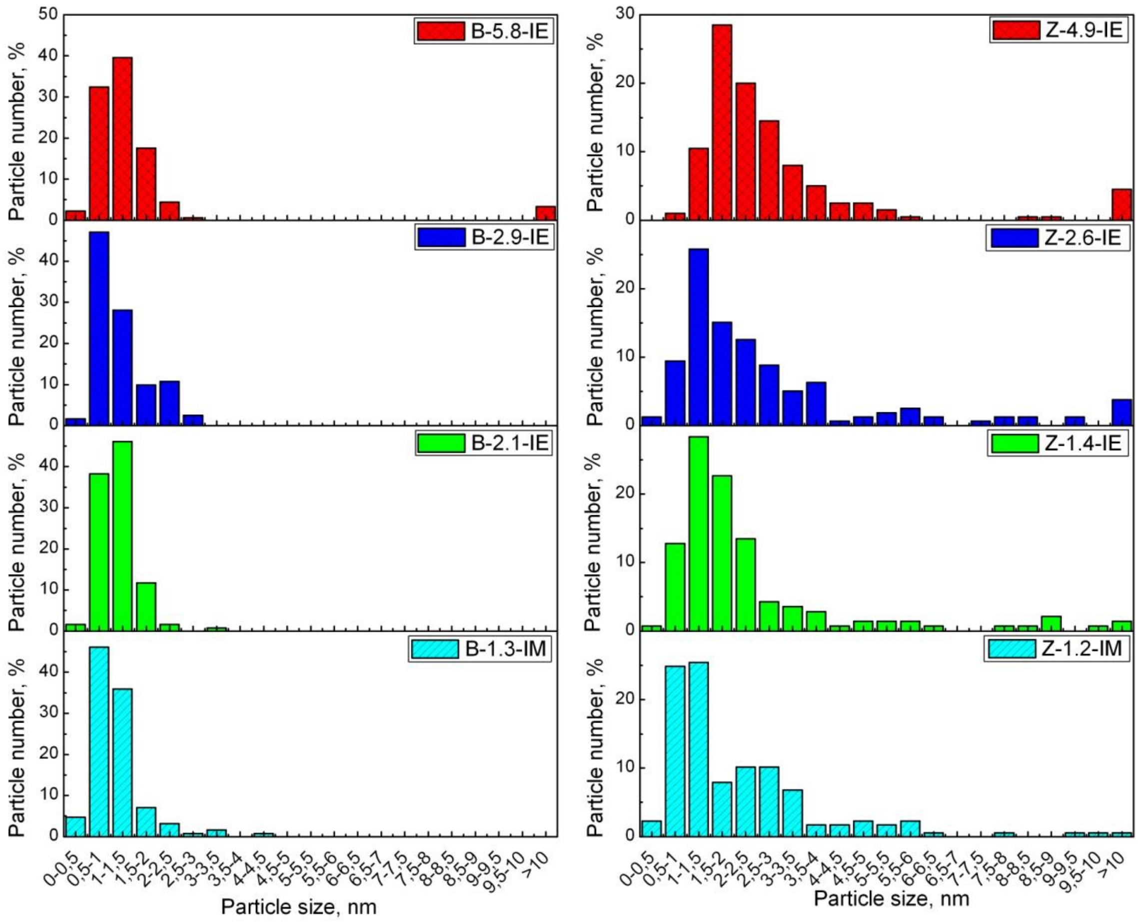
B-5.8-IE
B-2.9-IE
B-2.1-IE
B-1.3-IM
Z-4.9-IE
Z-2.6-IE
Z-1.4-IE
Z-1.2-IM
Particle number, %
Particle size, nm
0-0,5
0,5-1
1-1,5
1,5-2
2-2,5
2,5-3
3-3,5
3,5-4
4-4,5
4,5-5
5-5,5
5,5-6
6-6,5
6,5-7
7-7,5
7,5-8
8-8,5
8,5-9
9-9,5
9,5-10
>10

Figure 4

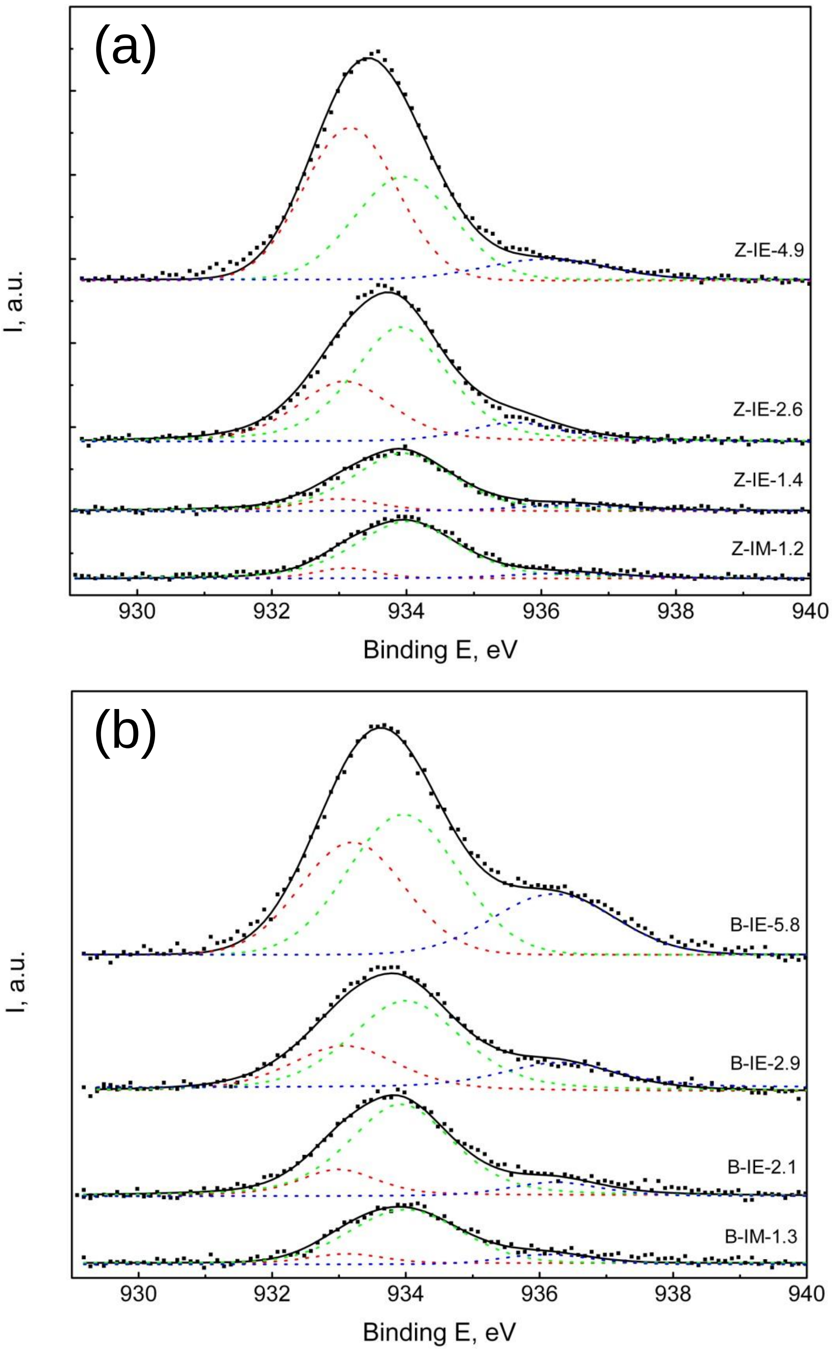
(a)
I, a.u.
Z-IE-4.9
Z-IE-2.6
Z-IE-1.4
Z-IM-1.2
930
932
934
936
938
940
Binding E, eV
(b)
I, a.u.
B-IE-5.8
B-IE-2.9
B-IE-2.1
B-IM-1.3
930
932
934
936
938
940
Binding E, eV

Figure 5

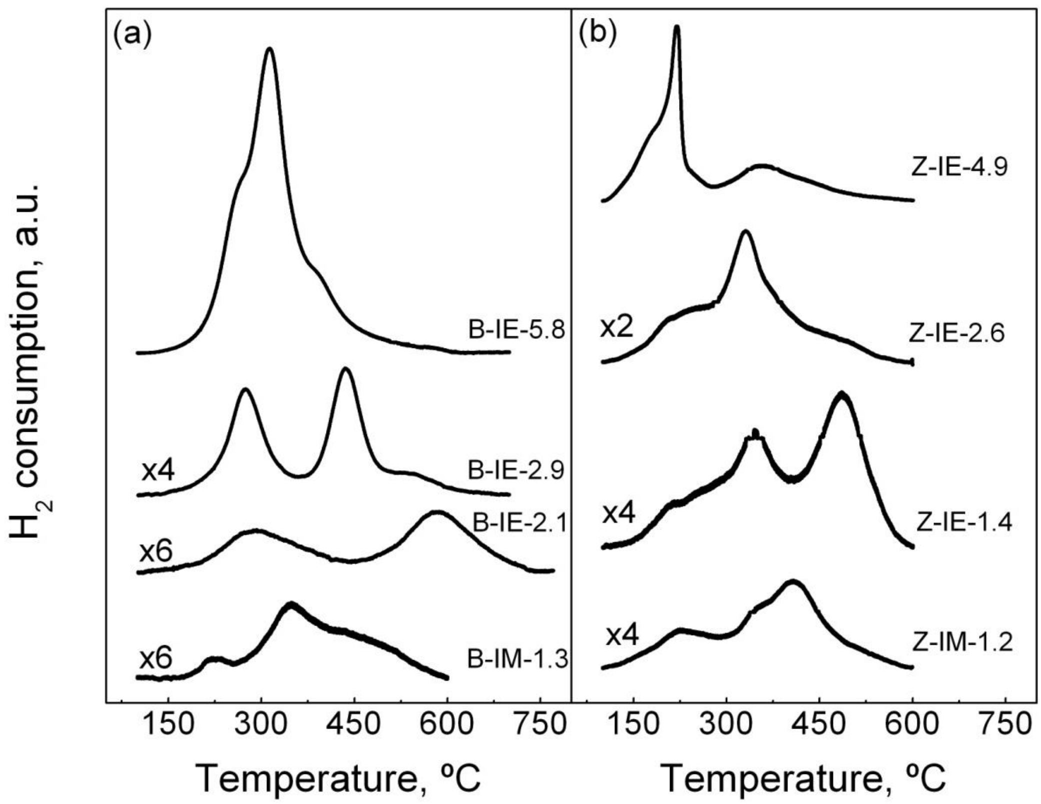
(a)
(b)
H_2 consumption, a.u.
B-IE-5.8
x4
B-IE-2.9
x6
B-IE-2.1
x6
B-IM-1.3
Z-IE-4.9
x2
Z-IE-2.6
x4
Z-IE-1.4
x4
Z-IM-1.2
150 300 450 600 750
Temperature, ºC
150 300 450 600 750
Temperature, ºC

Figure 6

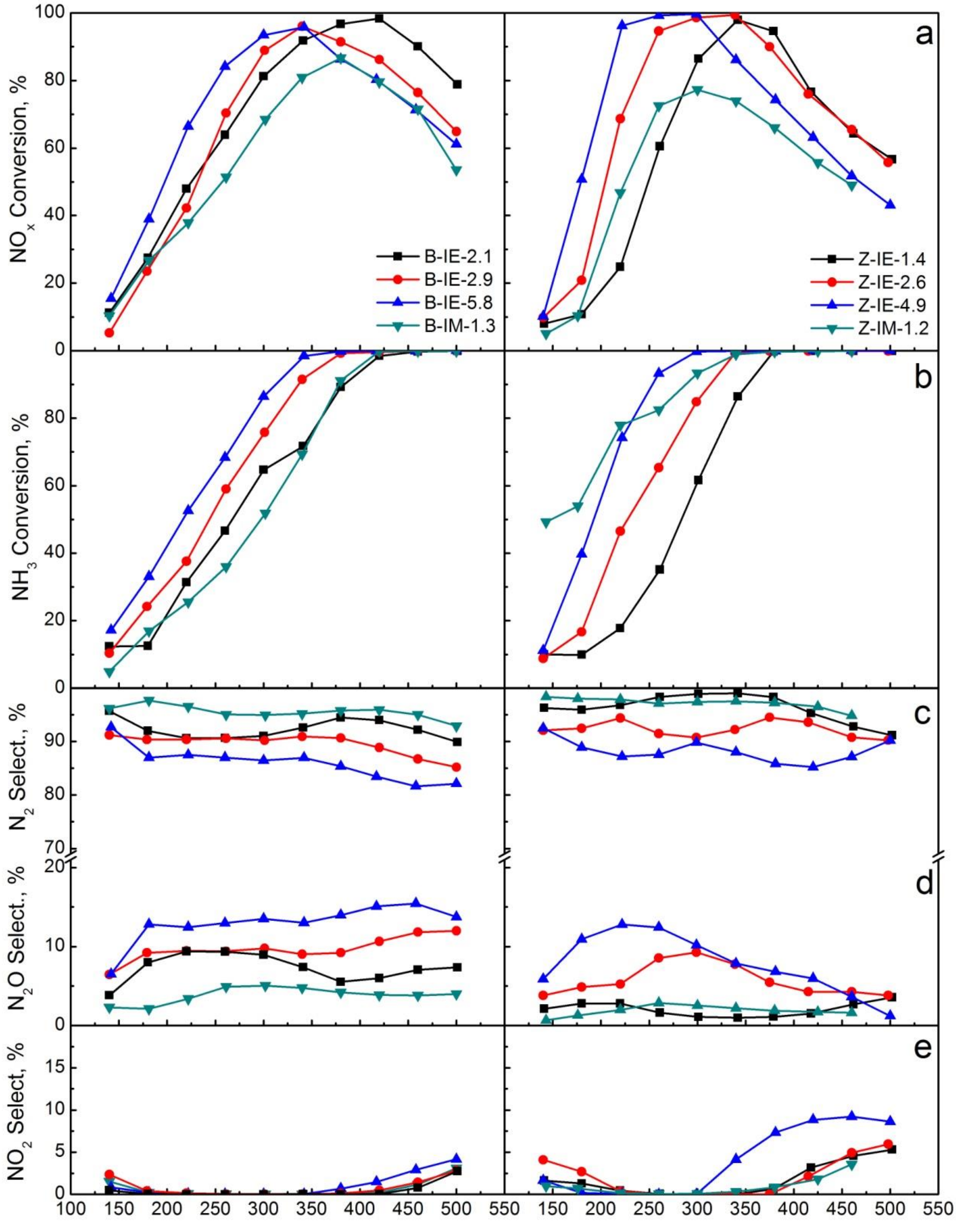

677

678

679 **Figure 7**